A robotic platform to screen aqueous two-phase systems for overcoming inhibition in enzymatic reactions

Bussamra, Bianca Consorti; Gomes, Joana Castro; Freitas, Sindelia; Mussatto, Solange I.; da Costa, Aline Carvalho; van der Wielen, Luuk; Ottens, Marcel

DOI
10.1016/j.biortech.2019.01.136

Publication date
2019

Document Version
Accepted author manuscript

Published in
Bioresource Technology

Citation (APA)
Bussamra, B. C., Gomes, J. C., Freitas, S., Mussatto, S. I., da Costa, A. C., van der Wielen, L., & Ottens, M. (2019). A robotic platform to screen aqueous two-phase systems for overcoming inhibition in enzymatic reactions. *Bioresource Technology*, *280*, 37-50. https://doi.org/10.1016/j.biortech.2019.01.136

A robotic platform to screen aqueous two-phase systems for overcoming inhibition in enzymatic reactions

Bianca Consorti Bussamra, Joana Castro Gomes, Sindelia Freitas, Solange I. Mussatto, Aline Carvalho da Costa, Luuk van der Wielen, Marcel Ottens

PII: S0960-8524(19)30169-5
DOI: https://doi.org/10.1016/j.biortech.2019.01.136
Reference: BITE 21013

To appear in: *Bioresource Technology*

Received Date: 5 December 2018
Revised Date: 27 January 2019
Accepted Date: 29 January 2019

Please cite this article as: Consorti Bussamra, B., Castro Gomes, J., Freitas, S., Mussatto, S.I., Carvalho da Costa, A., van der Wielen, L., Ottens, M., A robotic platform to screen aqueous two-phase systems for overcoming inhibition in enzymatic reactions, *Bioresource Technology* (2019), doi: https://doi.org/10.1016/j.biortech.2019.01.136

A robotic platform to screen aqueous two-phase systems for overcoming inhibition in enzymatic reactions

Bianca Consorti Bussamra[1, 2], Joana Castro Gomes[1], Sindelia Freitas[2], Solange I. Mussatto[3], Aline Carvalho da Costa[2], Luuk van der Wielen[1,4], Marcel Ottens[*,1]

[1]Department of Biotechnology, Delft University of Technology. Van der Maasweg 9, 2629HZ. Delft, The Netherlands.

[2]Development of Processes and Products (DDPP), University of Campinas. Av. Albert Einstein, 500. Post Code: 6066. Campinas, Brazil.

[3]Novo Nordisk Foundation Center for Biosustainability, Technical University of Denmark. Kemitorvet, Building 220. 2800, Kongens Lyngby, Denmark.

[4]Bernal Institute, University of Limerick. Castletroy. Limerick, Ireland.

Email addresses

Bianca Consorti Bussamra: b.consortibussamra@tudelft.nl

Joana Castro Gomes: joana.c.gomes@outlook.com

Sindelia Freitas: sindelia.freitas@gmail.com

Solange I. Mussatto: smussatto@biosustain.dtu.dk

Aline Carvalho da Costa: accosta@feq.unicamp.br

Luuk van der Wielen: L.A.M.vanderWielen@tudelft.nl

Marcel Ottens: M.Ottens@tudelft.nl

Abstract

Aqueous two-phase systems (ATPS) can be applied to enzymatic reactions that are affected by product inhibition. In the biorefinery context, sugars inhibit the cellulolytic enzymes in charge of converting the biomass. Here, we present a strategy to select an ATPS (formed by polymer and salt) that can separate sugar and enzymes. This automated and miniaturized method is able to determine phase diagrams and partition coefficients of solutes in these. Tailored approaches to quantify the solutes are presented, taking into account the limitations of techniques that can be applied with ATPS due to the interference of phase forming components with the analytics. The developed high-throughput (HT) platform identifies suitable phase forming components and the tie line of operation. This fast methodology proposes to screen up to six different polymer-salt

* Corresponding author: Dr. Marcel Ottens

systems in eight days and supplies the results to understand the influence of sugar and protein concentrations on their partition coefficients.

Keywords: aqueous two-phase system (ATPS); high-throughput screening; glucose partitioning; protein partitioning; product inhibition.

1. Introduction

The use of enzymes for a variety of processes has a significant role in industries. Generally, enzymes are applied to catalyse different type of reactions in food, animal feed, pharmaceutical, textile, pulp and paper and biofuel industries (Ogawa and Shimizu, 1999). Enzymatic reactions are also used to replace chemical routes, making processes more environmentally friendly (Margeot et al., 2009). For example, lignocellulosic materials, which are residues of agro-industries, can be converted into sugars by hydrolytic enzymes. In a biorefinery context, the efficiency of this reaction would contribute to the generation of renewable energy, which could reduce the usage of fossil fuels. Because more products can be generated from the same amount of (renewable) raw material, the productivity and possibilities to vary the portfolio of products in a biorefinery would be enhanced. Some studies claim that the enzymatic hydrolysis is the bottleneck in the conversion of lignocellulose to second generation ethanol and renewable sugars (Mesa et al., 2016). Thus, technologies to make enzymatic hydrolysis economically attractive have been a topic of much discussion in terms of operation mode, and load of solids and enzymes.

Product inhibition plays a significant role among the many obstacles that prevent enzymes to perform at their maximum activity (Modenbach and Nokes, 2013). Yang et al. (2011) demonstrated how the removal of end products was crucial to enhance the productivity of enzymatic hydrolysis. Thus, the inhibition by products can be overcome through an *in situ* removal of products during the reaction. In this work, we suggest aqueous two-phase systems (ATPS) as a strategy to separate sugars (product) and enzymes. Consequently, high sugar production could be achieved during hydrolysis of lignocellulosic material.

A wide range of studies have identified ATPS as an interesting technique to extract, separate, purify and concentrate substances (Iqbal et al., 2016). This type of system was first described by Albertsson (1961). Being formed by two immiscible components, named phase forming components, these systems constitute two aqueous phases that can unevenly partition

molecules, also called solutes, based on properties of both system and solutes (Baskir et al., 1989). A range of components can be used to form the different phases, such as two polymers, a polymer and a salt (Van Sonsbeek et al., 1993), or ionic liquids (Freire et al., 2012). Hence, both phases are mainly composed by water (79-90%), but each of them is enriched in a different component, which contributes to some advantages of ATPS, such as biocompatibility, simplicity and easy scale up (Phong et al., 2018). Moreover, ATPS presents a suitable environment to maintain enzymatic activity, as proved by Tjerneld et al. (1991), and has been already applied to biological processes involving laccase and further extraction of products and recovery of enzymes (Ferreira et al., 2018). Hence, an ATPS that can separate enzymes and sugar (reaction product) to opposite phases presents two main advantages: a friendly environment for enzymatic reaction and the *in situ* removal of products while they are released.

High-throughput (HT) platforms have gained attention in recent years in order to enable an automated and miniaturized experimental setup. Oelmeier et al. (2011), Diederich et al. (2013), Zimmermann et al. (2016) and Pirrung et al. (2018) demonstrated the improvements that a HT platform brings to the pharmaceutical field. In line with these authors, Bensch et al. (2007) also called the attention to the advantage of designing processes meanwhile screening a variety of parameters, which is offered by HT platforms. In the field of lignocellulose-to-biofuels, there are reported advances of HT techniques focused on pre-treatment, hydrolysis (Chundawat et al., 2008) and enzymatic assays (Goddard and Reymond, 2004). Selig et al. (2010) described a HT assay to perform hydrothermal pre-treatment of lignocellulosic material followed by enzymatic hydrolysis. The main outcomes of the automated and miniaturized technique of their research included the 96-well pre-treatment reactor, the direct use of the pre-treated slurry to enzyme saccharification and the solids handling system (Selig et al., 2010). Aiming to optimize biomass conversion, Chundawat et al. (2008) developed a HT platform to assess lignocellulosic digestibility. When conducting hydrolysis in a miniaturized scale, some parameters such as particle size, solid load, mass transfers and reaction time should be appropriately defined. However, delivering reproducible quantities of solids into micro-wells is an inherent problem of HT platforms. Other researches focused on the enzymatic assay developments — for example, the traditional filter paper assay to measure activity of cellulase was applied to an automated robotic platform (Decker et al., 2003). However, to the best of our knowledge, there is no

literature reporting the use of an automated and miniaturized robotic platform to determine phase diagrams and concentration of solutes in the phases (top and bottom), as well as solutions for the interference of system components on the analytics (e.g. in protein measurements), focusing to overcome inhibition of enzymatic reactions through ATPS.

This work aimed to develop a strategic methodology to screen and select ATPS able to separate sugar and hydrolytic enzymes. We found that both solutes (sugar and enzymes) could be quantified taking into account the interference of the phase forming components in the measurements. Then, this paper indicates a reliable manner to HT determine phase diagrams and partition coefficients in ATPS. Step by step of the developed strategy is presented, which was tested under different system components. Therefore, this platform provides the tools to overcome enzymatic inhibition, attributed to the reasonable selection of systems which are able to extract the product (inhibitors) from reaction medium. Integrating our novel technique with the available HT advances in the field of lignocellulose-to-biofuels, we provide tools to accelerate the development of feasible lignocellulose conversions.

2. Materials and Methods

2.1 Research Design

In this research, we developed a HT platform to screen ATPS formed by polymer and salt. The ATPS can be applied to conduct enzymatic reactions that are inhibited by products. Here, enzymatic hydrolysis of biomass was the reaction in focus. This reaction is catalyzed by hydrolytic enzymes that convert lignocellulosic biomass into sugars. The enzymes were represented by the enzymatic cocktail Cellic CTec (Novozymes). For simplification purpose, the addition of glucose simulated the degradation of the sugarcane bagasse by enzymes, since the substrate (bagasse) was not included in the screening experiments.

The development of this platform consisted of two main parts: determination of phase diagrams (binodal curves and tie lines) and quantification of the solutes (sugar and proteins) in both top and bottom phases. We chose the well-reported system composed of potassium phosphate buffer and poly (ethylene) glycol 2000 g/mol to establish the methodology for phase diagrams determination. In this part, the robotic platform generated a large number of points — consisted of different concentrations of phase forming components —, in order to detect the minimum number necessary to determine a precise binodal curve and tie lines. The definition of liquid

handling parameters (e. g. aspiration speed and delay, retract speed of the tips, dispense and breakoff speed, air gap sizes, aspiration and dispense positions) requires an extensive theoretical knowledge as well as trial and error tests. The parameters of aspiration and dispense applied to this work for each solution handled in the robotic platform facilitates its immediate application.

In the second part of the platform development, we evaluated analytical methods for quantification of the solutes. The platform presents an approach that takes into account the interference of the phase forming components in the analytics and is able to predict the protein quantification in a HT way. Six ATPS formed by the combination of different molecular weights of PEG (2000 g/mol,4000 g/mol and 6000 g/mol) and different salt types (potassium citrate and magnesium sulphate) illustrated the performance of the robotic platform. Hence, in a practical approach, we validated the feasibility of the platform.

2.2 Materials and stock solutions

Table 1 presents the reagents and components used with their supplier and purity, when applied. Polyethylene glycol 2000 g/mol with molar mass (PEG 2000), 4000 g/mol (PEG 4000), 6000 g/mol (PEG 6000) were dissolved in double distilled deionized water (Milli-Q water) to prepare the following stock solutions: 41 and 38% (w/w) PEG 2000, 41% (w/w) PEG 4000 and 31 and 39% (w/w) PEG 6000. The volumetric concentrations of stock solutions (grams of polymer per 100 mL of solution) were verified by a linear relation between density and concentration.

Stock solutions presented the final concentration of 40% (w/w) in Milli-Q water [buffer solutions were prepared at a final concentration of salts of 40% (w/w) in Milli-Q water], except for the salt solutions of sodium sulphate [25% (w/w)] and potassium citrate tribasic [50% (w/w)]. The pH was adjusted by adding sodium hydroxide (4 M) or hydrogen chloride, both purchased from Merck. Citrate buffer 50 mM was prepared by adding 10.505 g of citric acid monohydrate to a final volume of 1L Milli-Q water, already considering the volume of NaOH (4 M) used to correct the pH to 4.8.

The commercial enzyme Cellic CTec2 (Novozymes, Bagsværd, Denmark) presented an activity of 146 FPU/mL, measured according to the NREL protocol (Adney and Baker, 2008). Sugar solutions of different concentrations were prepared in Milli-Q water with anhydrous glucose.

Sodium carbonate (Na_2CO_3) and 3,5-Dinitrosalicylic acid (DNS) were used for enzymatic activities assays; and methyl violet, a hydrophobic dye, was used in the determination of phase diagrams in the HT platform.

2.3 Formation of ATPS

The automated determination of phase diagrams and partition coefficient of solutes was conducted at a Tecan Freedom Evo 200 platform equipped with one Liquid Handling Arm (LiHa), one Multi-Channel Arm™ (MCA), a robotic manipulator (RoMa) arm and an Infinite 200 PRO spectrophotometer (Tecan, Crailsheim, Germany). The systems were prepared by adding the required amounts of phase forming components in the 2 mL ninety-six deep well plates (Eppendorf, Hamburg, Germany). PEG solution was added first to each well (in a dry contact mode — tips in contact with the empty bottom of the recipient during liquid dispense), followed by Milli-Q water (in a free dispense mode — no contact of the tips with the recipient or another liquid during liquid dispense), and later the salt solution, which were dispensed through a wet contact mode (tips in contact with the liquids already present in the recipient during liquid dispense). The total working volume was established as 1 mL. Sugar and protein solutions (required in the partition coefficient experiments) were also added to the system by the liquid handling station. Information on source labware position, destination position, volume of pipetting and dispense and applied liquid class was defined per each solution and accessed by the EVOware system through worklists. The 96 systems formed into the deep well plate reached equilibrium by mixing on Eppendorf Thermomixer® C (plate adaptor SmartBlock) at 1300 rpm for 1 h at 21 °C for potassium phosphate and PEG 2000 systems (for the development of the binodal curve determination methodology) and 40 °C for all other systems. The target of the equilibrium tests (not shown) was to achieve constant partition coefficient of methyl violet in different ATPS. Even though literature evidences that 5 – 8 min is sufficient to mix ATPS containing methyl violet (Zimmermann et al., 2016; Oelmeier et al., 2011), we opted for a longer time (1 h), since the equilibrium tests were not performed for all the phase forming components screened. The plate was centrifuged for 30 min at 3000 rpm for phase separation (Eppendorf 5810R Multipurpose Centrifuge®). Both top and bottom phases were withdrawn and stored in order to perform the necessary analysis.

2.4 Manual binodal curve determination

The cloud point method (also called titrimetric method) (Kaul, 2000) was used in order to validate the data obtained in the robotic platform. This method determines the binodal curve by calculating the concentration of both phase forming components in the moment when a clear solution becomes turbid due to the addition of one phase solution to the other. The collection of several system points constituted the binodal curve.

2.5 HT phase diagram determination

Through the robotic platform, the determination of the binodal curve was conducted fitting a curve between the region of one-phase systems and two-phase systems. Ninety-six systems containing 50 µL of 1mM methyl violet were formed by the HT platform. The dye was pipetted by MCA 96. In order to construct the binodal curve, it was necessary to identify when each of the random systems was constituted by one or two phases by measuring the difference between the absorbance in the top phase and the bottom phase. In order to measure the content of methyl violet in both top and bottom phases, 30 µL of each phase were diluted 1:7 in appropriate solution to a final volume of 210 µL, in UV-Star® Microplates (Greiner Bio-One, Frickenhausen, Germany). After a mixing step (Eppendorf Thermomixer® C) for 1 min at 1000 rpm, the absorbance was measured at 586 nm. When the difference between absorbance of top and bottom phases was below a cut-off value of 0.113 (586 nm), the system was defined as monophasic.

The binodal curve from both manual and robotic measurements were determined by fitting the data points corresponding to one and two-phase systems to an empirical curve developed by Merchuk, (1998), represented below:

$$c_{\text{polymer}} = \text{A} \cdot \exp[\left(\text{B} \cdot c_{\text{salt}}^{0.5}\right) + (\text{C} \cdot c_{\text{salt}}^{3})]. \quad (1)$$

The terms c_{polymer} and c_{salt} are the polymer and the salt concentrations, respectively, expressed in weight percentage. A, B and C are the fitting parameters obtained by least squares regression. This non-linear regression was performed with Matlab® R2018b using the function *lsqcurvefit* (The Mathworks, Natrick, ME, USA).

For tie lines determination, the lever arm rule was applied. The composition of top and bottom phases of a specified system (M point) can be inferred by the intersection between the tie line and the binodal curve (Diederich et al., 2013). The lever arm rule correlates the ratio between top phase volume (V_{tp}) and bottom phase volume (V_{bp}) to the distance between the M point and

(2)

the points in the binodal curve that represents the composition of both top and bottom phases (L_{bp} and L_{tp}, respectively).

$$\frac{V_{\mathrm{tp}}}{V_{\mathrm{bp}}} = \frac{L_{\mathrm{bp}}}{L_{\mathrm{tp}}}.$$

The following equations were used to determine the composition of top and bottom phases, as established by Diederich et al. (2013).

$$c_{\mathrm{PEG}}^{\mathrm{tp}} - f\left(c_{\mathrm{salt}}^{\mathrm{tp}}\right) = 0 \quad (3)$$

$$c_{\mathrm{PEG}}^{\mathrm{bp}} - f\left(c_{\mathrm{salt}}^{\mathrm{bp}}\right) = 0 \quad (4)$$

$$\frac{\left(c_{\mathrm{salt}}^{\mathrm{bp}} - c_{\mathrm{salt}}^{\mathrm{M}}\right)^2 + \left(c_{\mathrm{PEG}}^{\mathrm{M}} - c_{\mathrm{PEG}}^{\mathrm{bp}}\right)^2}{\left(c_{\mathrm{salt}}^{\mathrm{M}} - c_{\mathrm{salt}}^{\mathrm{tp}}\right)^2 + \left(c_{\mathrm{PEG}}^{\mathrm{tp}} - c_{\mathrm{PEG}}^{\mathrm{M}}\right)^2} - \left(\frac{V_{\mathrm{tp}}}{V_{\mathrm{bp}}}\right)^2 = 0 \quad (5)$$

$$\frac{c_{\mathrm{PEG}}^{\mathrm{bp}} - c_{\mathrm{PEG}}^{\mathrm{M}}}{c_{\mathrm{salt}}^{\mathrm{bp}} - c_{\mathrm{salt}}^{\mathrm{M}}} - \frac{c_{\mathrm{PEG}}^{\mathrm{M}} - c_{\mathrm{PEG}}^{\mathrm{tp}}}{c_{\mathrm{salt}}^{\mathrm{M}} - c_{\mathrm{salt}}^{\mathrm{tp}}} = 0 \quad (6)$$

Equations (3) and (4) represent the tie line intersections with binodal curve. The points of the binodal curve are represented by $f\left(c_{\mathrm{salt}}^{\mathrm{tp}}\right)$ and $f(c_{\mathrm{salt}}^{\mathrm{bp}})$, respectively for top and bottom phases. Equation (5) applies the Pythagorean Theorem for two triangles, in which the line of segments L_{tp} and L_{bp} represent the hypotenuses. Then, the tie line is determined when the slopes of the hypotenuses are equal, as defined in Equation (6). Each tie line was determined using a different M point.

The tie line length (TLL) was calculated according to the following equation:

$$TLL = \sqrt{\left(c_{\mathrm{PEG}}^{\mathrm{tp}} - c_{\mathrm{PEG}}^{\mathrm{bp}}\right)^2 - \left(c_{\mathrm{salt}}^{\mathrm{tp}} - c_{\mathrm{salt}}^{\mathrm{bp}}\right)^2}. \quad (7)$$

2.6 Phase Volume determination

Both binodal curve and tie lines can be determined with the same set of data. In this research, it was found that a salt concentration lower than 2% (w/w) greatly influenced the absorbance of methyl violet, while the polymer (PEG) concentration did not interfere. Thus, for the tie line determination, samples of the top and bottom phases were diluted in a solution of 2% (w/w) salt. Consequently, each salt system requires its own calibration curve of methyl violet.

As the methyl violet partitions in both top and bottom phases for certain system compositions, the determination of phase volumes was based on the mass balance of the dye in the system and the assumption that the volume of the phase is equal to the total volume of the system, as presented in the equations below:

$$C_{\mathrm{MV,\,stock}}.V_{\mathrm{MV}} = C_{\mathrm{MV,tp}}.V_{\mathrm{tp}} + C_{\mathrm{MV,\,bp}}.V_{\mathrm{bp}} \quad (8)$$

$$V_{\mathrm{tp}} + V_{\mathrm{bp}} = 1\ \mathrm{mL}. \quad (9)$$

Concentration of methyl violet in the bottom and top phases ($C_{\mathrm{MV,\,bp}}$ and $C_{\mathrm{MV,\,top}}$, respectively) were calculated according to the methyl's violet calibration curve. The $C_{\mathrm{MV,\,stock}}$ and V_{MV} are the concentration of methyl violet stock solution and the corresponding volume added into the system, respectively. V_{tp} and V_{bp} are the volumes of top and bottom phases to be calculated. The non-linear system of equations (Equations 3, 4, 5, 6, 8 and 9) was solved iteratively using *fsolve* operation in Matlab® R2018b (The MathWorks, Natick, ME, USA).

2.7 Partitioning of solutes in HT platform

In order to assess how the concentration of the phase forming components and solutes influence the partition of sugar and enzymes in ATPS, different tie line lengths were tested for different concentrations of sugar and enzymes. Solutes partitioning was evaluated separately, since the presence of different concentrations of sugar in the system could affect the accuracy of the enzymatic activity assay, and the sugar-enriched enzymatic cocktail could contribute to an error in the sugar quantification — the glucose concentration in Cellic CTec2 is 250 ± 8 g/L; at the highest protein load experiment (15 FPU/g bagasse), 2.6 ± 0.1 g/L glucose was present in the system. HT quantification of protein and sugar in top and bottom phases was validated by mass balance for the total amount of these solutes in the system.

The glucose concentrations were defined considering the expected conversion capacity of the system and the inhibitory sugar concentration. For a maximum theoretical conversion of biomass, at 10% solid load, the concentration of sugar would be approximately 90 g/L. However, the reaction can be inhibited from a sugar concentration of 27 g/L on. Then, systems containing 28 g/L ± 0.5, 29 g/L ± 0.3, 51 g/L ± 0.5 and 61 g/L ± 0.6 of sugar were performed.

The definition of the enzyme concentration took into consideration reported values of enzyme loads for hydrolysis and the profitability of the process, since the biocatalyst contributes to a substantial part of the operational costs in a biorefinery (Torres, 2016). The enzyme load was calculated based on 5, 10 and 15 FPU/g bagasse, considering a (hypothetical) substrate load of 10% (WIS — water insoluble substrate). Taking into account a working volume of 1 mL, 0.1 g of dry biomass would be expected in each reaction. The volume of enzymatic cocktail to be added to the system was calculated as follows:

$$V_{\mathrm{enz}} = \frac{10\ (\mathrm{FPU/g}) \cdot m_{\mathrm{dry\ bag}}}{FPAse_{\mathrm{cocktail}}}, \quad (10)$$

where $FPAse_{\text{cocktail}}$ is the total enzymatic activity of the commercial cocktail (146 FPU/mL).

To fulfil the requirements of the liquid handling minimum volume, the stock solution was diluted according to the load of each experiment and to maintain a fixed volume of enzyme preparation of 68 µL and sugar preparation of 92 µL for all systems.

2.8 Analytical methods

The analytical methods for protein quantification, total cellulose activity and sugar quantification are presented below.

2.8.1 Protein quantification

Absorbance at 280 nm and Bradford assay were evaluated for protein quantification. In order to obtain a reliable protein quantification, two main aspects were considered. First, the enzymatic cocktail may not partition equally through the system — especially components other than proteins. In order to evaluate the influence of these contaminants, an ultrafiltration of the enzymatic cocktail was performed using 3.000 MWCO Amicon® Ultra Centrifugal Filters, as described by the supplier. Retentate (target protein solution) and permeate (contaminants) were evaluated through each protein method (absorbance at 280 nm and Bradford assay). Finally, special attention should be paid to the influence of phase forming components on the absorbance in the wavelength used for each method.

Protein quantification of top and bottom phases was performed using the Coomassie Protein Assay Reagent (Thermo Scientific, USA) (Bradford, 1976). The reaction was performed according to the method provided by the supplier. In this case, 250 µL of Bradford reagent were added, using the MCA arm, to each well of the reaction plate for protein quantification already containing 10 µL of sample, blanks and internal standards.

The phase forming components (and their dilutions) influence the absorbance on Bradford method (González-González et al., 2011). Therefore, the absorbance measurement for each sample was corrected with the corresponding blank presenting the same dilution factor (DF).

For the determination of protein concentration, an internal standard (STD) containing a known protein concentration was prepared for each system composition — respecting the same influence of phase forming components for samples and internal standards. Then, sample concentrations were determined by

$$C_{\text{sample}} = \frac{Abs^{\alpha}_{\text{sample}}\, DF_{\text{sample}}}{Abs^{\alpha}_{\text{std}}\, DF_{\text{std}}} C_{\text{std}}, \tag{11}$$

where the concentration of the enzyme in the top or bottom phase (α) is given by the ratio between the absorbance of the sample ($Abs_{\text{sample}}^{\alpha}$) and the absorbance of the internal standard enzyme solution ($Abs_{\text{std}}^{\alpha}$), both corrected by the respective dilution factors (DF), multiplied by the known concentration of the internal standard enzyme solution (C_{std}). Absorbance of both samples and internal standards was corrected by subtracting a blank for each system composition.

2.8.2 Filter paper activity (FPAse)

The total cellulase activity in terms of filter paper units (FPU) was measured by reducing in 10 times the scale of the NREL method (Adney and Baker, 2008). The colour development and sugar quantification were carried out according to the method proposed by Miller (1959).

2.8.3 Sugar quantification

Sugar concentration in the top and bottom phases of ATPSs was determined using the Megazyme Glucose Reagent assay (Megazyme, Wicklow, Irland). Samples were diluted in Mili-Q water prior to quantification assay, in order to obtain the measurement in the linearity range of the calibration curve. The reaction, which consisted of 200 µL of the Megazyme Glucose Reagent and 10 µL of sample, was incubated for 10 min at 37 °C and the absorbance read at 505 nm. A calibration curve in the range of 1 to 12 mM glucose was prepared. It was proved that the phase forming components did not influence the quantification method (data not shown). Then, only one blank (composed of water) was enough to complete the set of reaction needed for this quantification protocol. Samples were aspirated and dispensed with the LiHa fixed tips, while Glucose reagent buffer was added to the UV plates containing the diluted samples with MCA 96.

2.9 Relative sugar release

The relative sugar release is the correlation of the enzymatic activity in two different conditions (Moreira et al., 2013). In one condition (control assay), 50 µL of enzymes were incubated at 50 ºC, 1300 rpm for 30 min with 100 µL of citrate buffer (50 mM pH 4.8). Simultaneously, the enzymes (50 µL) were incubated with the phase forming constituents [100 µL salts at 10% (w/w) solution], for the same period of time and temperature. After the incubation time, 7.5 mg of Whatman grade 1 filter paper substrate (GE Healthcare, Chicago, IL) were added to both solutions, and the reaction was carried out at 50 ºC, static condition, for 60 min. After diluting

the systems with 100 µL of Mili-Q water, the sugar release was measured by Megazyme Glucose Reagent assay.

2.10 Enzymatic hydrolysis

The hydrolysis of sugarcane bagasse was conducted for two purposes: identification of the sugar inhibitory concentration and assessment of protein adsorption to sugarcane bagasse. At a scale of 1.5 mL final volume, the hydrolysis was conducted at 10% (w/v) water-insoluble substrate (WIS), pH 4.8 (50 mM citrate buffer), and 0.02% azide monosodic. The reaction was incubated at 50 ºC and 1300 rpm (Eppendorf Thermomixer C). The protein load was established at 10 FPU per gram of bagasse (Cellic CTec2 145 FPU/mL). For the sugar inhibition experiments, 10 g/L, 20 g/L, 40 g/L and 60 g/L glucose were added to the reaction media before the hydrolysis. For adsorption experiments, no external sugars were added to the reaction. Sampling was performed at 6, 12, 24 and 48 h for inhibitory sugar experiments and at 3, 6, 24 and 48 h of reaction time for protein adsorption experiments. To stop the enzymatic activity, samples were centrifuged (4000 rpm at 4 ºC) for 10 min. Supernatants were collected and analysed for sugar and protein contents, and enzymatic activities, according to conditions described above. For the experiment of sugar inhibitory concentration, samples were boiled at 95 ºC for 10 min after being collected, to ensure no remaining enzymatic activity and sugar production.

2.11 Data analysis

The TLL experimental data were correlated using Othmer-Tobias (Othmer and Tobias, 1942), which is presented by

$$\left(\frac{1-C_{\mathrm{PEG}}^{\mathrm{tp}}}{C_{\mathrm{PEG}}^{\mathrm{tp}}}\right)=K_{\mathrm{OT}}\left(\frac{1-C_{\mathrm{Salt}}^{\mathrm{bp}}}{C_{\mathrm{Salt}}^{\mathrm{bp}}}\right). \tag{12}$$

The linear dependency of the plots $\log\left(\frac{1-c_{\mathrm{p,\,tp}}}{c_{\mathrm{p,\,tp}}}\right)$ against $\log\left(\frac{1-c_{\mathrm{s,\,bp}}}{c_{\mathrm{s,\,bp}}}\right)$, and $\log\left(\frac{c_{\mathrm{w,\,bp}}}{c_{\mathrm{s,\,bp}}}\right)$ against $\log\left(\frac{c_{\mathrm{w,\,tp}}}{c_{\mathrm{p,\,tp}}}\right)$ iindicates an acceptable consistency of the results.

The standar deviation (σ) and correlation coefficient (r^2) for all correlated data were calculated by the following formulas (Press et al., 2007), respectevely: $\sigma=\sqrt{\sum_{i=1}^{N}(y_i-f(x_i))^2/N-k}$ and

$r^2 = 1 - \sum_{i=1}^{N}(y_i - f(x_i))^2 \Big/ \sum_{i=1}^{N}(y_i - \overline{y})^2$, where N is the number of point used for the regression, and k is the number of parameters.

The partition coefficient in a two-phase system can be determined as the ratio of enzyme/sugar concentration in the top phase to that in the bottom phase (Li et al., 2002).

The uncertainties of the measurements calculated by calibration curves were estimated by the formula $\partial_{meas} = \frac{S_r}{m} \cdot \sqrt{\frac{1}{M} + \frac{1}{N} + \frac{(y_{meas} - \overline{y})^2}{m^2 \cdot SS_x}}$ (Barwick, 2003), where S_r represents the residual standard deviation of the calibration curve, m is the slope of the curve, M is the number of paired calibration points, N is the number of replicates made on the sample, y_{meas} is the measured value calculated by the calibration curve, $\overline{y}$ is the mean of the measured values (y) used to estimate the calibration curve and SS_x is the sum of squares of deviation of the independent values (x_i data points) from the mean of the x_i values ($SS_x = \sum_{i=1}^{n}(x_i - \overline{x})^2$). The errors were propagated accordingly. Measurements presenting the standard deviation within the 95% confidence interval are indicated in the text. In this case, the uncertainty (∂_{meas}) was multiplied by the 2-tailed Student *t* value for 95% level of confidence and *n-2* degrees of freedom connected to the respective calibration curve.

3. Results and Discussion

A strategy to screen and select ATPS for enzymatic reactions, aiming at the partition of product (glucose) and enzyme (protein) to different phases, is presented. This strategy consists of two sequential sections. The first section aims to select phase forming components based on their capability to offer enzymes a suitable environment to release glucose from filter paper. The performance of the enzymes in each phase forming components was compared with their performance when incubated in optimum condition (citrate buffer, 50 mM pH 4.8). The ratio of sugar released under both conditions gives the relative sugar release of the enzymes. This indicator guided the preselection of suitable phase forming components in terms of maintenance of enzymatic activity. Then, the ones which presented a satisfactory response in this step were selected to be studied in the second section of the described methodology.

Then, in Section 2, we suggest the use of the automated and miniaturized robotic platform developed, which is applied to select biphasic systems that can separate enzymes and sugars

unevenly between the phases. Through phase diagrams and partition coefficients of solutes, it is possible to select the most suitable ATPS for our application.

3.1 Development of the HT platform

The developed HT screening platform gives information to determine phase diagrams for different phase forming components (e.g.: polymer molecular weight and salt types) and evaluates the interference of parameters (e.g.: concentration of phase forming components and solutes) in the partition coefficient of the solutes in a short time. Moreover, the scale of each experiment and volume of reactants can be reduced when compared to a manual approach. However, the majority of the techniques regarding the obtainment of binodal curves and tie lines in literature considers a manual approach and is not compatible with HT screening (Bensch et al., 2007). Here, we discuss the methodological differences of published platforms for HT screening of ATPS and the one developed in this work, in terms of equilibrium achievement, two phase system identification and tie lines determination.

3.1.1 Binodal determination

To determine the binodal curves, points representing mono and biphasic systems in the boarder of the phase transition were used for the regression of parameters to fit to the Merchuk equation (Merchuk et al., 1998b). The developed robotic platform determines whether there are one or two phases. For the system PEG/phosphate investigated by Bensch et al. (2007), the addition of methyl violet enabled the identification of phases. The colorful component partitions equally in monophasic systems, or to the top phase when the system is biphasic. In this work, however, it was noted that the hydrophobic marker partitioned unevenly to both phases in some two-phase systems. Then, the identification was dependent on the difference in concentration of methyl violet in top and bottom phases. Some authors suggest a visual inspection (Zimmermann et al., 2016) or an identification based on the cloud point method (Oelmeier et al., 2011) to determine the two phase systems. Although these approaches save reactants (no dye is needed), the binodal curve and tie lines cannot be determined with the same dataset, and an additional experiment has to be performed to phase volume determination.

By comparing the difference in absorbance, given by the experiment and the visual inspection for 343 systems, a cut-off value of 0.1137 was selected to represent the transition between mono and biphasic systems formed by potassium phosphate and PEG 2000. In this study, a

step of 1% (w/w) in the composition of each point was performed (Fig. 1.a). The data generated by the HT method were compared to the results of the manual approach. The HT binodal curve fits in the region within 95% confidence interval of the manual dataset, validating the HT methodology (Fig. 1.b). Moreover, the points obtained by the HT curve differ in 9.9%[1] in relation to the manual values (absolute deviation). Oelmeier et al. (2011) also proved that both liquid handling system and manual approach generated binodal data points for PEG 4000 and PO_4 that fall within the 95% prediction bounds of the fitted curve determined by the combination of both data sets.

There are some limitations to distinguish between mono and biphasic systems in highly concentrated systems. For monophasic systems containing high salt concentrations (hydrophilic systems), methyl violet can partition as a separate phase to the walls of the plate. Consequently, the surface of the systems is not homogeneous. Depending on the position of the tips during the withdrawal of the top phase, a deceptive identification of a biphasic system could occur. For systems with high polymer concentrations, the viscosity of the medium could impede the partition of methyl violet, leading to inaccurate results. Moreover, the increase of the molecular weight of the polymer leads to a larger biphasic region above the binodal curve (Iqbal et al., 2016). Therefore, the experimental space indicated in Table 2 was defined according to the molecular weight of the PEG and the effect of it on the binodal curve position.

In order to reduce the number of data points used to binodal curve determination (in one plate, 96 systems can be performed), steps of 2.4% (w/w) for both polymer and salt (defined as data 1 in Fig. 2), and 2% (w/w) for salt and 1% (w/w) for polymer (defined as data 2 in Fig. 2) were performed for systems composed by potassium sodium tartrate pH 7 (

Fig. 2.a) and potassium citrate pH 7 (

Fig. 2.b), both with PEG 6000. The absolute deviation of the binodal curve obtained at 2.4% (w/w) step in relation to the curves obtained within a more narrow step of concentration [2% (w/w) salt and 1% (w/w) PEG] was 1.3%[1] and 14.8%[1] for the systems with potassium sodium tartrate and potassium citrate, respectively. The comparison (in absolute deviation) of the phase diagrams demonstrates that steps up to 2.4% (w/w) in phase components concentration still

[1] $AAD = \frac{1}{K}\sum_{i=1}^{k}\left(\left(\frac{c_{PEG,\,manual} - c_{PEG,HTS}}{c_{PEG,\,manual}}\right)^2\right)^{0.5}$, for the independent variable C_{salt} being 7%, 9%, 11%, 13%, 15%, 17% (w/w).

lead to an accurate binodal curve for screening purposes. Then, depending on the maximum mass concentration of the polymer and salt, defined according to Table 2, steps varying from 1% (w/w) to 2.4% (w/w) can be applied. Variation of phase forming components in steps up to 0.25% (w/w) is reported in literature, which leads to high precision of the binodal curve (Zimmermann et al., 2016). However, in order to obtain valuable data for the phase diagram determination when using smaller concentration steps, initial guesses have to be accurate, otherwise the experiments might need to be repeated.

3.1.2 Tie lines determination

The tie lines determination method was tested for the systems potassium sodium tartrate pH 7 and potassium citrate pH 7, both with PEG 6000. As the tie line represents a range of polymer-salt composition with common partition coefficient, they should be determined at hydrolysis temperature — 50 °C. However, due to equipment limitations, 40 °C was the highest temperature at which mixing and centrifugation could be operated. After reaching the equilibrium (mixing and phase separation) at 40 °C, the temperature of the system did not influence the partitioning of the solute methyl violet (data not shown).

The lever arm rule requires the composition of one point (M point) per tie line to be determined. By fixing the salt concentration, points presenting different PEG concentrations would lie on different tie lines. In the phase diagram shown in Fig. 2, a fixed concentration of salt was used for all M points. The tie lines determined for the system potassium citrate pH 7 and PEG 6000 (Fig. 2.d) took into account two different sets of salt concentration. For both systems, the higher the polymer concentration of the M point, the more unreliable the tie line was. This is indicated by tie lines crossing each other in this region, probably because of the logarithm shape of the binodal curve, leading to a scattered determination of salt concentration in the bottom phase. Then, high polymer concentrated region should be avoided in the phase diagram determination. Moreover, obtaining a suitable tie line to separate protein and sugar at low concentration of components is more interesting at an economic perspective as well.

The Othmer-Tobias (Othmer and Tobias, 1942) correlation indicate the consistency of the determined tie lines. Excluding the last tie line for the system with potassium citrate pH 7, the correlation presented an R-square of 0.97. The same behaviour is observed in the potassium

sodium tartrate system: when the last two tie lines were excluded, the r-square increased 16.45%.

The determination of phase volumes neglected the difference of densities in top and bottom phases. However, the density is linearly correlated to the concentration of compounds — and the effect of concentration in density is stronger to salts than to polymers (data not shown). Then, for systems with high mass concentrations of salt and polymer, the difference in phase densities is more pronounced. Not taking into account the influence of phase forming concentration on the density of the phases introduces an error in the volume determination. Diederich et al. (2013) estimated an error of about 1 to 7% in the phase concentrations when neglecting the difference in phase densities in the lever arm rule. We consider this error acceptable for screening purposes.

3.1.3 Solute quantification in ATPS

In order to develop a reliable platform to calculate partition coefficients of solutes, quantifications methods for sugars and enzymes were evaluated. The components of the enzymatic cocktail Cellic CTec2 other than proteins, taken as the permeated of ultrafiltration, represents 27.3% of the absorbance of the cocktail at 280 nm. Since we cannot predict the even partition of these components with the proteins in the ATPS, this method could lead to miscalculation in protein quantification. Contrarily, the permeate fraction does not present signal in Bradford method, being this method selected to quantify proteins. Phase forming components did not interfere with the glucose quantification method. However, the method selected to quantify protein (Bradford) took into account the interference of phase forming components with the reagent.

The accuracy of the Bradford assay can be influenced by the presence of polyethylene glycol. Barbosa et al. (2009) demonstrated that the concentration of the polymer interferes in the absorbance readings of the protein-dye complex. For example, the absorbance of 25 µg/mL protein solution can be up to 80% lower in 40% (w/w) polymer. When diluted in 10% (w/w) polymer, the same protein concentration exhibits a 15% reduction in absorbance at 595 nm (A_{595}). According to Bradford (1976), the influence by nonprotein components can be overcome by considering a control with the same solution composition of the samples. However, high polymer concentrations [> 10% (w/w)] decrease the sensitivity of the method. Thus, low protein

concentrations could not be detected, even when calibration curves are prepared with the same polymer concentrations (Barbosa et al., 2009). In this research, the Bradford method determines the protein concentration of two times diluted samples of top and bottom phases. Then, even systems containing 20% (w/w) polymer initially would present an appropriate concentration to lead to accurate results. However, proteins were also diluted, possibly implying low sensitivity measurements.

3.1.4 Summary of the HT platform

Dividing the HT screening platform in three steps gives a convenient way to apply this methodology (Fig. 3). In the first step, 96 different compositions of the same polymer-salt system are generated. These systems, classified as mono or biphasic, provide information for binodal curve determination. Moreover, the volumes of top and bottom phases for the biphasic system can be calculated. These data support the determination of tie lines. Two plates can be generated and processed per day, totalizing three days to generate the phase diagrams for 6 polymer-salt systems.

Different tie lines regions and different concentration of the solutes can be explored in the robotic platform. In the second step of the platform, eight different compositions of each polymer-salt combination are assessed in terms of their ability to partition sugar and enzymes. The selection of these system compositions is arbitrary and depends on the goals of the research. In this work, we selected compositions that represent moderate concentration of phase forming components (i. e., systems presenting similar top and bottom phases and close to the binodal curve). The lower the concentration of phase forming components, the lower the viscosity of the system. Less viscous systems are easier to operate, which also increases their accuracy of results. Each deep-well plate can support the study of two polymer-salt combinations, containing eight different composition of phase forming component each. For six polymer-salt combinations, three days are necessary to perform the experiments and analyse the data.

The concentrations of solutes (enzyme and sugar) can vary according to the stage of the enzymatic hydrolysis. End-products of the reaction (sugar) inhibit both the catalytic site of the enzymes and the adsorption of them to the substrate, at high solid concentrations (Kristensen et al., 2009). After 6 hours of reaction, 76 ± 4.4% (95% confidence interval) of the protein load was

adsorbed to the bagasse. In the end of the reaction (48h), this value increased to 85 ± 4.7% (95% confidence interval). Thus, the largest contribution to different concentration of proteins in hydrolysis reaction can be attributed to the enzyme load choice. On the other hand, the proteins would never be 100% adsorbed, since the cocktail presents an amount of non-binding enzymes (Kristensen et al., 2009), and not all proteins measured are enzymes. Regarding the sugars, the maximum glucose concentration was 43 ± 2.5 g/L (49 ± 3% cellulose conversion), achieved after 48 h of reaction without the presence of external inhibitory sugar. After 6h reaction, 62% of the sugar was produced (27 ± 1 g/L glucose). This concentration can be considered inhibitory and one of the causes that levels off the conversion rate of the reaction. Kristensen et al. (2009) suggested that above a certain glucose concentration (known as glucose level threshold), enzymes are inhibited to a similar extent. However, the presence of additional glucose in the beginning of the reaction promotes a reduction of the initial rate. Consequently, the hydrolysis would take more time to achieve the same conversion as the hydrolysis without the inhibitor at the initial time. In the presence of 60 g/L glucose in the medium, the initial conversion rate is prominently lower.

In order to design a process for enzymatic reactions in ATPS, it is important to take into account the variation of solute concentration in time. In step 3, up to six systems can be assessed regarding the influence of glucose and enzymes concentrations on their own partition coefficient. Some authors assessed the influence of parameters (e.g. pH, NaCl and tie line length) in HT platforms via Design of Experiments (DoE) (Oelmeier et al., 2011). Here, we opted to screen a broader combination of parameters, since these data can be further used for modelling of phase formation and solute partitioning in ATPS. The move to step 3 is selective, since only the systems presenting the most different partition coefficient ratio in step 2 are selected to be further studied. Additionally, step 3 could involve the determination of specific enzymatic activity, assessing the partition of the different enzymes (cellobiohydrolase, xylanase and β-glucosidase) of the cocktail in the phases. Two days are reserved for step 3, summing up eight days to perform the complete and integrated platform.

As a result of these experiments, the most suitable tie lines (concentration of PEG and salt) can be selected. Even though the systems that lay on the same tie line present similar partition coefficients, these systems can be different in terms of volume phase ratio and total

concentration of the components (Hatti-kaul, 2001). As a consequence, the most suitable volume phase ratio can be selected when defining the process and the total concentration of components based on economic issues. Then, not only the partition coefficients of sugar and enzymes were considered to select the systems, but also other characteristics, such as the vulnerability of the system close to the binodal curve or critical point, the accordance of the phase volume ratio with further purification steps and the ease to scale up the process.

3.2 Section 1: pre-selection of components for ATPS

The strategy to select suitable ATPS that can partition sugar and enzymes was applied to three polymer weights and eleven types of salts. The salt types were pre-selected based on their influence over enzymatic activities. In this way, the sugar (from the substrate filter paper) released by enzymes was measured in each phase forming component. The system potassium citrate pH 7 with PEG 6000 presented during the development of the HT platform was evaluated in order to assess the pH influence in the sugar release. The salt solutions potassium citrate pH 5.0 and magnesium sulphate pH 5.0 provided the medium where enzymes could release the highest sugar concentration. They represent around 50% of the sugar released in the optimum conditions (citrate buffer 50 mM).

3.3 Section 2: Application of the HT platform

Six systems comprising three different polymer molecular weights (2000, 4000 and 600 g/mol) and two types of salts (magnesium sulphate and potassium citrate) were evaluated in the developed HT platform regarding their ability to partition sugar and enzymes.

3.3.1 Determination of phase diagrams (step 1)

Binodal curves for each system are shown in Fig. 4. Following the determination of the binodal curves in the HT station, tie lines were calculated. Tie line construction was based on the lever arm rule, which considers the system composition, the empirical binodal curve and the volume ratio between phases.

Polymer of higher molecular weight promotes a shift of the binodal curve towards the origin of the phase diagram, increasing the two-phase region (Fig. 4.a, Fig. 4.b and Fig. 4.c for potassium citrate pH 5; and Fig. 4.d, Fig. 4.e and Fig. 4.f for magnesium sulphate pH 5). As a consequence, low components concentrations are required to form a two phase system composed by high molecular weight polymer. Low concentration of phase forming components

is interesting because of costs reduction and ease to recycle back to the process. On the other hand, high molecular weight polymers are viscous, which can make their handling more difficult and decrease their volume accuracy in the system.

Increasing the pH shifts the binodal curve toward the origin (Fig. 4.c and Fig. 2.d). Due to the four dissociation constants presented by the citric acid, the pH significantly influences the anion species in solution for the systems composed by potassium citrate. At pH 7, almost 100% of the species in solution are trivalent, while at pH 5 the majority of species in solution (approximately 70%) are divalent (Heller et al., 2012). The increase in anion charge leads to a higher polarizability and a more stable ion-dipole salt-PEG interactions. In consequence, less concentration of components is required to form. The significant difference in slope and shape of the binodal curve due to pH change was also observed for the system composed by PEG 1000 and phosphate salt (Diederich et al., 2013). Even though two phase systems can be achieved with lower concentrations of phase forming components at higher pH, the enzymatic reaction aimed to be conducted in ATPS is pH-dependent. Therefore, the enzymatic activity is considered more important than the components (salt-PEG) concentrations.

3.3.2 Influence of the ATPS composition on solute partitioning (Step 2)

After the construction of the phase diagrams for each polymer-salt combination, the partitioning of sugar and enzymes in the systems was evaluated. In step 2, the influence of the tie line length (salt-polymer mass concentration) on the partition of solutes was assessed for each polymer-salt combination (Fig. 5). A fixed concentration of glucose and enzymes were added to the systems and top and bottom phases were measured. Mass balances for the total amount of solute in the systems show the accuracy of the measurements. This validation could also be done by comparing the partition coefficient obtained by HT and manual approaches (Oelmeier et al., 2011). However, we considered the mass balance of the solute sufficient to validate our methodology.

Because of the high partition coefficient of enzymes, the systems PEG 2000 – magnesium sulphate and PEG 6000 – potassium citrate presented the most distinct partition coefficient of solutes. The partition of proteins to the polymer-enriched top phase can be justified by the salting out effect promoted by the ionic strength of the system. In this work, potassium citrate systems promoted a higher salting out effect when compared to the magnesium sulphate

system. This is in agreement with the previous finding of (Wiendahl et al., 2009), who reported the precipitation of proteins — as a result of the salting out effect — being more prominent for the citrate than to the sulphate anion. However, these anions were both prepared as sodium salts. If we analyze the Hofmeister series, both salts (potassium citrate and magnesium sulphate) present very similar concentration at the precipitation limit (Kunz et al., 2004). Okur et al. (2017) investigated the molecular level of interaction between proteins and salts. The different types of enzymes in this work make the prediction of the salt effect on proteins according to the Hofmeister series even more ingenious. Then, this leads to the conclusion that other effect is acting as the main driving force to the partition of proteins in these systems. Andrews and Asenjo (2010) mentioned the hydrophobicity as a key factor in determining the partition of proteins in polymer-salt ATPS. The higher the polymer molecular weight, the higher the hydrophobicity of the top phase. This can justify the larger partition of proteins (charged molecules) to the top phase in the system formed by PEG 6000. However, the increase in TLL reduces the free volume available for the protein (Suarez et al., 2018), leading to an exclusion effect of the proteins towards the opposite salt enriched phase. The partition of proteins observed in this work shows an opposite tendency, since the partition coefficient of these molecules increase with the increasing the TLL for the majority of the systems (Fig. 5).

3.3.3 Influence of solute concentration on solute partitioning (Step 3)

The influence of sugar and enzymes concentrations on their partitioning in the systems was assessed in step 3. Here, only the polymer-salt system and its respective tie lines (6 ATPS in total) that presented the most distinct partition coefficient of solutes in Step 2 were studied. Partition coefficients of sugar and enzymes were determined at 3 different concentrations of these solutes and in 3 different concentrations of the polymer-salt (tie line lengths). The concentration of proteins influenced their partition more significantly for the systems composed by PEG 6000 and potassium citrate. In this line, the partition coefficient tends to decrease when the load of protein increases (Fig. 6.a). This could be explained by the low solubility of protein with increase of its concentration, leading to precipitation to the bottom phase. The systems formed by PEG 2000-magnesium sulphate pH 5 presented partition coefficients of enzymes close to the unity; however, the more concentrated in the system, the higher the partition regardless the load of protein (Fig. 6.b).

Comparing these results with those obtained in Step 2, although they follow similar tendency, the partition coefficient of proteins differs. Considering that the methodology was improved along with the first application of the platform, results of Step 3 should be taken as more reliable (Table 3). Internal standards for Steps 2 and 3 were composed under different strategies. While in Step 2 the internal standard was composed by CellicCTec 10 times diluted, in Step 3 the CelliCTec was diluted 30 or 50 times before being added to compose the internal standard. With the latter approach, we could avoid aggregation of proteins and depletion of the free dye at high protein concentrations during quantification (Barbosa et al., 2009).

The partition coefficients of sugar are not highly influenced by the concentration of that solute (sugar) in the system (Fig. 6.c and Fig. 6.d). However, K_s tend to decrease at high concentrations of sugar (60 g/L), for both systems and tie lines assessed. This means that sugar concentrates at the bottom phase when the concentration of this solute in the system is getting close to the saturation concentration. On the other hand, the sum of sugar present in top and bottom phase deviates more from the total mass added when the tie line is higher (Table 4). This could be a consequence of inaccuracy in the determination of volumes when the systems are more concentrated in phase forming components, as mentioned before. Moreover, we could also assume losses of solutes at the interface that are not being quantified in the top and bottom phases, contributing to the larger deviations. Thus, the higher mass balance deviation of certain systems should not be exclusively associated to an inaccurate quantification of the solutes in these systems. For the system composed by PEG 6000-potassium citrate pH5, the mass balance deviations are in general bigger, indicating that the loss of solutes at the interface could be more pronounced to that system. A high salting out effect can also lead to protein precipitation at the interface (Benavides et al., 2011). However, the higher deviation in mass balance occurred when the solutes concentration was increased. This suggests that the higher concentration of solutes is more likely to cause partition to the interface than higher polymer and salt concentrations (higher TLL), probably due to the solubility limit of protein in salts (Wiendahl et al., 2009).

The results obtained in one run of the platform indicate that the ATPS composed by PEG 6000-potassium citrate pH 5 is suitable to the separation of sugar and proteins. Although sugar was almost evenly partitioned to the phases, this feature can be overcome according to the mode of

operation of the hydrolysis reaction (e.g. continuously removing of bottom phase or a counter-current system). The high partition coefficient of proteins reveals the potential of this system to separate enzymes. By partitioning enzymes and products to different phases, both reaction and extraction of products can coexist in the same system. Partition of the bagasse to the top phase and maintenance of the enzymatic activity would confirm the application of this system to the enzymatic hydrolysis of cellulose.

4. Conclusion

The proposed strategy comprehensively screens and selects ATPS to conduct extractive enzymatic reactions. The systems are selected in terms of the phase components that maintain the enzymatic activity and unevenly partition enzymes and sugar to different phases. Associated to the computational solution of equations, the developed robotic platform determines phase diagrams for polymer-salt systems and partition coefficient of solutes under influence of different parameters of interest. Conceptually, when conducted in an extractive mode, the enzymatic reactions that were previously inhibited by products tend to maintain their maximum activities and highly feasible enzymatic processes could be designed using ATPS.

Appendix for Supplementary data

E-supplementary data of this work can be found in the online version of the paper.

Acknowledgement

This work was financially supported by the Foundation for Research of State of Sao Paulo, Brazil [grant numbers 2015/20630-4, 2016/04749-4, 2016/06142-0 and BEPE 2016/21951-1]; and the BE-Basic Foundation, The Netherlands. This research was carried out during a Dual Degree PhD program under agreement between UNICAMP and TU Delft. The authors thank Yi Song for assisting with the TECAN platform and Marcelo Henriques da Silva, for all inputs to the platform development and data analysis.

Conflict of interest

The authors have no competing interests to declare.

References

1. Adney, B., Baker, J., 2008. Measurement of Cellulase Activities Laboratory Analytical Procedure (LAP) Issue Date : 08 / 12 / 1996, National Renewable Energy Laboratory (NREL).

2. Albertsson, P.-Å., 1961. Fractionation of particles and macromolecules in aqueous two-phase systems. Biochem. Pharmacol. 5, 351–358. https://doi.org/10.1016/0006-2952(61)90028-4

3. Andrews, B.A., Asenjo, J.A., 2010. Theoretical and experimental evaluation of hydrophobicity of proteins to predict their partitioning behavior in aqueous two phase systems: A review. Sep. Sci. Technol. 45, 2165–2170. https://doi.org/10.1080/01496395.2010.507436

4. Barbosa, H., Slater, N.K.H., Marcos, J.C., 2009. Protein quantification in the presence of poly(ethylene glycol) and dextran using the Bradford method. Anal. Biochem. 395, 108–110. https://doi.org/10.1016/j.ab.2009.07.045

5. Barwick, V., 2003. Preparation of Calibration Curves. A guide to Best Practice.

6. Baskir, J.N., Hatton, T.A., Suter, U.W., 1989. Protein partitioning in two-phase aqueous polymer systems. Biotechnol. Bioeng. 34, 541–558. https://doi.org/10.1002/bit.260340414

7. Benavides, J., Rito-Palomares, M., Asenjo, J.A., 2011. Aqueous Two-Phase Systems, Second Edi. ed, Comprehensive Biotechnology. Elsevier B.V. https://doi.org/10.1016/B978-0-08-088504-9.00124-0

8. Bensch, M., Selbach, B., Hubbuch, J., 2007. High throughput screening techniques in downstream processing: Preparation, characterization and optimization of aqueous two-phase systems. Chem. Eng. Sci. 62, 2011–2021. https://doi.org/10.1016/j.ces.2006.12.053

9. Bradford, M.M., 1976. A rapid and sensitive method for the quantitation of microgram quantities of protein utilizing the principle of protein-dye binding. Anal. Biochem. 72, 248–254. https://doi.org/10.1016/0003-2697(76)90527-3

10. Chundawat, S.P.S., Balan, V., Dale, B.E., 2008. High-throughput microplate technique for enzymatic hydrolysis of lignocellulosic biomass. Biotechnol. Bioeng. 99, 1281–1294. https://doi.org/10.1002/bit.21805

11. Decker, S.R., Adney, W.S., Jennings, E., Vinzant, T.B., Himmel, M.E., 2003. Automated Filter Paper Assay for Determination of Cellulase Activity. Appl. Biochem. Biotechnol. 105–108, 689–703.

12. Diederich, P., Amrhein, S., Hammerling, F., Hubbuch, J., 2013. Evaluation of PEG/phosphate aqueous two-phase systems for the purification of the chicken egg white protein avidin by using high-throughput techniques. Chem. Eng. Sci. 104, 945–956. https://doi.org/10.1016/j.ces.2013.10.008

13. Ferreira, A.M., Passos, H., Okafuji, A., Tavares, A.P.M., Ohno, H., Freire, M.G., Coutinho, J.A.P., 2018. An integrated process for enzymatic catalysis allowing product recovery and enzyme reuse by applying thermoreversible aqueous biphasic systems. Green Chem. 20, 1218–1223. https://doi.org/10.1039/C7GC03880A

14. Freire, M.G., Cláudio, A.F.M., Araújo, J.M.M., Coutinho, J. a. P., Marrucho, I.M., Lopes, J.N.C., Rebelo, L.P.N., 2012. Aqueous biphasic systems: a boost brought about by using ionic liquids. Chem. Soc. Rev. 41, 4966. https://doi.org/10.1039/c2cs35151j

15. Goddard, J.P., Reymond, J.L., 2004. Enzyme assays for high-throughput screening. Curr. Opin. Biotechnol. 15, 314–322. https://doi.org/10.1016/j.copbio.2004.06.008

16. González-González, M., Mayolo-Deloisa, K., Rito-Palomares, M., Winkler, R., 2011. Colorimetric protein quantification in aqueous two-phase systems. Process Biochem. 46, 413–417. https://doi.org/10.1016/j.procbio.2010.08.026

17. Hatti-kaul, R., 2001. Aqueous Two-Phase Systems. Mol. Biotechnol. 19, 269–177.

18. Heller, A., Barkleit, A., Foerstendorf, H., Tsushima, S., Heim, K., Bernhard, G., 2012. Curium(III) citrate speciation in biological systems: A europium(III) assisted spectroscopic and quantum chemical study. Dalt. Trans. 41, 13969–13983. https://doi.org/10.1039/c2dt31480k

19. Iqbal, M., Tao, Y., Xie, S., Zhu, Y., Chen, D., Wang, X., Huang, L., Peng, D., Sattar, A., Shabbir, M.A.B., Hussain, H.I., Ahmed, S., Yuan, Z., 2016. Aqueous two-phase system (ATPS): an overview and advances in its applications. Biol. Proced. Online 18, 18. https://doi.org/10.1186/s12575-016-0048-8

20. Kaul, A., 2000. Chapter 2: The Phase Diagram, in: Hatti-Kaul, R. (Ed.), Methods in Biotechnology. Aqueous Two-Phase Systems. pp. 11–21. https://doi.org/10.1385/1-59259-028-4:11

21. Kristensen, J.B., Felby, C., Jørgensen, H., 2009. Yield-determining factors in high-solids enzymatic hydrolysis of lignocellulose. Biotechnol. Biofuels 10, 1–10. https://doi.org/10.1186/1754-6834-2-11

22. Kunz, W., Henle, J., Ninham, B.W., 2004. “Zur Lehre von der Wirkung der Salze” (about the science of the effect of salts): Franz Hofmeister’s historical papers. Curr. Opin. Colloid Interface Sci. 9, 19–37. https://doi.org/10.1016/j.cocis.2004.05.005

23. Li, M., Kim, J.W., Peeples, T.L., 2002. Amylase partitioning and extractive bioconversion of starch using thermoseparating aqueous two-phase systems. J. Biotechnol. 93, 15–26. https://doi.org/10.1016/S0168-1656(01)00382-0

24. Margeot, A., Hahn-Hagerdal, B., Edlund, M., Slade, R., Monot, F., 2009. New improvements for lignocellulosic ethanol. Curr. Opin. Biotechnol. 20, 372–380. https://doi.org/10.1016/j.copbio.2009.05.009

25. Merchuk, J.C., Andrews, B.A., Asenjo, J.A., 1998a. Aqueous two-phase systems for protein separation Studies on phase inversion. J. Chromatogr. B 711, 285–293.

26. Merchuk, J.C., Andrews, B.A., Asenjo, J.A., 1998b. Aqueous two-phase systems for protein separation Studies on phase inversion. J. Chromatogr. B 711, 285–293.

27. Mesa, L., López, N., Cara, C., Castro, E., González, E., Mussatto, S.I., 2016. Techno-economic evaluation of strategies based on two steps organosolv pretreatment and enzymatic hydrolysis of sugarcane bagasse for ethanol production. Renew. Energy 86, 270–279. https://doi.org/10.1016/j.renene.2015.07.105

28. Miller, G.L., 1959. Use of Dinitrosalicylic Acid Reagent for Determination of Reducing Sugar. Anal. Chem. 31, 426–428.

29. Modenbach, A.A., Nokes, S.E., 2013. Enzymatic hydrolysis of biomass at high-solids loadings - A review. Biomass and Bioenergy 56, 526–544. https://doi.org/10.1016/j.biombioe.2013.05.031 Review

30. Moreira, S., Silvério, S.C., Macedo, E.A., Milagres, A.M.F., Teixeira, J.A., Mussatto, S.I., 2013. Recovery of Peniophora cinerea laccase using aqueous two-phase systems composed by ethylene oxide / propylene oxide copolymer and potassium phosphate salts. J. Chromatogr. A 1321, 14–20. https://doi.org/10.1016/j.chroma.2013.10.056

31. Oelmeier, S.A., Dismer, F., Hubbuch, J., 2011. Application of an aqueous two-phase systems high-throughput screening method to evaluate mAb HCP separation. Biotechnol. Bioeng. 108, 69–81. https://doi.org/10.1002/bit.22900

32. Ogawa, J., Shimizu, S., 1999. Microbial enzymes: New industrial applications from traditional screening methods. Trends Biotechnol. 17, 13–21. https://doi.org/10.1016/S0167-7799(98)01227-X

33. Okur, H.I., Hladílková, J., Rembert, K.B., Cho, Y., Heyda, J., Dzubiella, J., Cremer, P.S.,

Jungwirth, P., 2017. Beyond the Hofmeister Series: Ion-Specific Effects on Proteins and Their Biological Functions. J. Phys. Chem. B 121, 1997–2014. https://doi.org/10.1021/acs.jpcb.6b10797

34. Othmer, D.F., Tobias, P.E., 1942. Liquid -Liquid Extraction Data -Toluene and Acetaldehyde Systems. Ind. Eng. Chem. 34, 690–692. https://doi.org/10.1021/ie50390a011
35. Phong, W.N., Show, P.L., Chow, Y.H., Ling, T.C., 2018. Recovery of biotechnological products using aqueous two phase systems. J. Biosci. Bioeng. xx. https://doi.org/10.1016/j.jbiosc.2018.03.005
36. Pirrung, S.M., Parruca da Cruz, D., Hanke, A.T., Berends, C., Van Beckhoven, R.F.W.C., Eppink, M.H.M., Ottens, M., 2018. Chromatographic parameter determination for complex biological feedstocks. Biotechnol. Prog. https://doi.org/10.1002/btpr.2642
37. Press, W., Teukolsky, S., Vetterling, W., Flannery, B., 2007. Numerical Recipes. The Art of Scientific Computing, Third Edit. ed. Cambridge University Press.
38. Selig, M.J., Tucker, M.P., Sykes, R.W., Reichel, K.L., Brunecky, R., Himmel, M.E., Davis, M.F., Decker, S.R., 2010. Lignocellulose recalcitrance screening by integrated high-throughput hydrothermal pretreatment and enzymatic saccharification. Ind. Biotechnol. 6, 104–111. https://doi.org/10.1089/ind.2010.0009
39. Suarez, E., Suarez, C.A., Tilaye, T., Eppink, M.H.M., Wij, R.H., Berg, C. Van Den, 2018. Fractionation of proteins and carbohydrates from crude microalgae extracts using an ionic liquid based-aqueous two phase system. Sep. Puri fi cation Technol. 204, 56–65. https://doi.org/10.1016/j.seppur.2018.04.043
40. Tjerneld, F., Persson, I., Lee, J.M., 1991. Enzymatic cellulose hydrolysis in an attrition bioreactor combined with an aqueous two-phase system. Biotechnol. Bioeng. 37, 876–882. https://doi.org/10.1002/bit.260370912
41. Torres, G.B., 2016. Decision Making at Early Design Stages: Economic Risk Analysis of Add-On Processes to Existing Sugarcane Biorefineries. University of Campinas.
42. Van Sonsbeek, H.M., Beeftink, H.H., Tramper, J., 1993. Two-liquid-phase bioreactors. Enzyme Microb. Technol. 15, 722–9. https://doi.org/http://dx.doi.org/10.1016/0141-0229(93)90001-I
43. Wiendahl, M., Olker, C., Husemann, I., Krarup, J., Staby, A., Scholl, S., Hubbuch, U., 2009.

A novel method to evaluate protein solubility using a high throughput screening approach. Chem. Eng. Sci. 64, 3778–3788. https://doi.org/10.1016/j.ces.2009.05.029

44. Yang, J., Zhang, X., Yong, Q., Yu, S., 2011. Three-stage enzymatic hydrolysis of steam-exploded corn stover at high substrate concentration. Bioresour. Technol. 102, 4905–4908. https://doi.org/10.1016/j.biortech.2010.12.047

45. Zimmermann, S., Gretzinger, S., Schwab, M.-L., Scheeder, C., Zimmermann, P.K., Oelmeier, S.A., Gottwald, E., Bogsnes, A., Hansson, M., Staby, A., Hubbuch, J., 2016. High-throughput downstream process development for cell-based products using aqueous two-phase systems. J. Chromatogr. A 1464, 1–11. https://doi.org/10.1016/j.chroma.2016.08.025

Figure Captions

Fig. 1. a) Classification of mono and biphasic systems based on the difference in absorbance at 586 nm between top and bottom phases. Analysis of 343 compositions of the phase forming components potassium phosphate and PEG 2000, at 21 °C. b) Comparison between binodal curve determined through HT and manual experiments. Both approached had the points fit to the Merchuk equation (Merchuk et al., 1998b). Manual curve parameters obtained by least square regression: $\mathbf{A = 0.8369, B = -5.344}$, $\mathbf{C = -113.6}$, $\mathbf{r^2 = 0.9598}$, $\boldsymbol{\sigma = 0.0157}$. HT curve parameters obtained by least square regression: $\mathbf{A = 0.6261, B = -4.091}$, $\mathbf{C = -239.8}$, $\mathbf{r^2 = 0.9867}$, $\boldsymbol{\sigma = 0.0106}$.

Fig. 2. Binodal curves determined for potassium sodium tartrate pH 7 (a) and potassium citrate pH 7 (b), both with PEG 6000 and at 40 °C, with their respective phase diagrams (c) and (d). The binodal curves were determined with two different spaces between points: 2.4% (w/w) for both salt and PEG (data 1); and 2% (w/w) for salt and 1% (w/w) for PEG (data 2). The pair of points representing a mono and a biphasic systems was fit to the Merchuk equation (Merchuk et al., 1998b). The regression parameters are: $\mathbf{A = 0.5811, B = -3.884, C = -167.4}$, $\mathbf{r^2 = 0.9474}$, $\boldsymbol{\sigma = 0.0177}$ for PEG 6000 and potassium sodium tartrate (data 1); $\mathbf{A = 0.4784, B = -3.135, C = -199.1}$, $\mathbf{r^2 = 0.9649}$, $\boldsymbol{\sigma = 0.0104}$ for PEG 6000 and potassium sodium tartrate (data 2); $\mathbf{A = 13.094, B = -16.206, C = 173.752}$, $\mathbf{r^2 = 0.9469}$, $\boldsymbol{\sigma = 0.0151}$ for PEG 6000 and potassium citrate (data 1); $\mathbf{A = 4.6971, B = -12.8231}$, $\mathbf{C = 163.478}$, $\mathbf{r^2 = 0.9606}$, $\boldsymbol{\sigma = 0.0089}$ for PEG 6000 and potassium citrate (data 2). For tie lines calculation, M points at 14% (w/w) of salt were used for potassium sodium tartrate, and 9% (w/w) and 12% (w/w) for potassium citrate.

Fig. 3. Schematic diagram of the robotic platform for ATPS screening. The three steps that compose the platform are represented in terms of experimental setup, analyses and results. In eight days, six polymer-salts can be screened. Step 1 involves the determination of phase diagrams for each polymer-salt system. In step 2, the influence of the phase forming concentration (represented as tie line length) on the partition coefficient of sugar (horizontal wells) and proteins (vertical wells) is evaluated. The systems that present the most distinct partition coefficient of solutes are selected to step 3. In this stage, up to 6 systems can be

assessed regarding the influence of sugar and protein concentration in their partition coefficient. The deep-wells distinguished inside the black rectangles represent the same ATPS (polymer-salt combination and concentration).

Fig. 4. Phase diagrams (binodal curves and tie lines) determined via HT experiments for systems containing two types of salts (potassium citrate pH 5 and magnesium sulphate pH 5) and different molecular weights of PEG (2000, 4000 and 6000 g/mol). The binodal data for all cases showed a good correlation (lowest r^2 was 0.9321), indicating that the experimental data is well described by the empirical equation.

Fig. 5. Influence of the system composition in the partitioning of sugar and enzymes. The x-axis was fixed at the same range to facilitate comparison.

Fig. 6. Influence of solute concentration on their partition coefficients in different tie line lengths (TLL). Effect of protein load (5, 10 and 15 FPU/g bagasse) on protein partition coefficient (Kp) for ATPS composed by PEG 6000 – potassium citrate pH 5 (a) and PEG 2000 – magnesium sulphate pH 5 (b). Points indicated with asterisk (*) presented absorbance of bottom phase below the intercept error obtained from the calibration curve. In this case, the maximum detectable concentration of protein in the bottom phase was used to calculate the partition coefficient (K_p), which can be the value indicated (*) or higher. Effect of sugar load (30, 50 and 60 g/L) on sugar partition coefficient (Ks) for ATPS composed by PEG 6000 – potassium citrate pH 5 (c) and PEG 2000 – magnesium sulphate pH 5 (d).

Tables

Table 1. List of reagents and components used in the development of the HT platform, as well as their supplier and respective purities.

Reagents and components	Supplier	Purity
Polyethylene glycol 2000 g/mol	Merck (Darmstad, Germany)	-
Polyethylene glycol 4000 g/mol	Merck (Darmstad, Germany)	-
Polyethylene glycol 6000 g/mol	J.T. Baker (Fisher, New Jersey, USA)	-
Potassium citrate tribasic monohydrate ($K_3C_6H_5O_7.H_2O$)	Sigma Aldrich (Taufkirchen, Germany)	≥ 99 %
Potassium sodium tartrate tetrahydrate ($KNaC_4H_4O_6.4H_2O$)	Sigma Aldrich (Taufkirchen, Germany)	≥ 99 %
Sodium phosphate monobasic dehydrate ($NaH_2PO_4.2H_2O$)	Sigma Aldrich (Taufkirchen, Germany)	≥ 95 %
Ammonium citrate dibasic ($(NH_4)_3C_6H_5O_7$)	Honeywell Fluka (Buchs, Switzerland)	≥ 99 %
Sodium tartrate dehydrate ($Na_2C_4H_4O_6.2H_2O$)	Sigma Aldrich (Taufkirchen, Germany)	≥ 99 %
Magnesium sulphate heptahydrate ($MgSO_4.7H_2O$)	J.T. Baker (Fisher, New Jersey, USA)	-
Potassium dihydrogen phosphate (KH_2PO_4)	Merck (Darmstad, Germany)	≥ 99 %
Sodium sulphate (Na_2SO_4)	Merck (Darmstad, Germany)	≥ 99 %
Potassium phosphate dibasic (K_2HPO_4)	Honeywell Fluka (Buchs, Switzerland)	≥ 99 %
Sodium succinate dibasic hexahydrate ($Na_2C_4H_6O_4.6H_2O$)	Sigma Aldrich (Taufkirchen, Germany)	≥ 99 %
Potassium oxalate monohydrate ($K_2C_2O_4.H_2O$)	Honeywell Fluka (Buchs, Switzerland)	≥ 99 %
Tri-Sodium citrate dihydrate ($Na_3C_6H_5O_7.2H_2O$)	Merck (Darmstad, Germany)	≥ 99 %
Anhydrous glucose	Sigma Aldrich (Taufkirchen, Germany)	-
Sodium carbonate (Na_2CO_3)	Sigma Aldrich (Taufkirchen, Germany)	≥ 99 %
3,5-Dinitrosalicylic acid (DNS)	Sigma Aldrich (Taufkirchen, Germany)	≥ 98 %
Methyl violet	Merck (Darmstad, Germany)	-

Table 2. Range of salt and polymer concentrations used to determine phase diagrams (at 40 °C) in the HT platform.

PEG MW	Reliable experimental area	
	Salt [% (w/w)]	Polymer [% (w/w)]
2000	10 to 25	3 to 25
4000	5 to 19	3 to 25
6000	1 to 20	1 to 25

Table 3. Deviation of the protein mass measured in top and bottom phase in relation to the total mass of protein added in the system (mass balance deviation), for different tie line lengths (TLL). The measured protein concentration was 0.3 g/L ± 0.03, 0.6 g/L ± 0.03 and 0.9 g/L ± 0.06, respectively to the enzymatic loads of 5, 10 and 15 PFU/g bagasse. The values are represented in percentage.

Protein load (FPU/g bagasse)	PEG 6000-potassium citrate pH5			PEG 2000-magnesium sulphate pH5		
	TLL 34.2 %	TLL 35.9%	TLL 38.1%	TLL 38.0%	TLL 40.2%	TLL 42.2%
5	29 ± 8	17 ± 8	15 ± 8	27 ± 7	27 ± 7	29 ± 8
10	41 ± 5	44 ± 5	48 ± 5	27 ± 4	32 ± 4	39 ± 5
15	47 ± 5	46 ± 5	56 ± 5	39 ± 5	35 ± 5	49 ± 5

Table 4. Deviation of the sugar mass measured in top and bottom phase in relation to the total mass of sugar added in the system (mass balance deviation), for different tie line lengths (TLL). The values are represented in percentage.

Sugar load (g/L)	PEG 6000-potassium citrate pH5			PEG 2000-magnesium sulphate pH5		
	TLL 34.2 %	TLL 35.9%	TLL 38.1%	TLL 38.0%	TLL 40.2%	TLL 42.2%
29 ± 0.3	9 ± 4	6 ± 4	15 ± 4	3 ± 4	2 ± 4	1 ± 4
51 ± 0.5	21 ± 2	37 ± 3	34 ± 3	14 ± 2	16 ± 2	16 ± 2
61 ± 0.6	28 ± 3	34 ± 3	38 ± 3	13 ± 4	7 ± 2	11 ± 4

Highlights

- The high-throughput platform developed can accelerate scientific findings in ATPS.
- Up to 6 ATPS can be fully determined within 8 days using the developed platform.
- Phase diagram and partition coefficient are sufficient to select extractive ATPS.
- PEG 6000 and potassium citrate systems partition cellulase mainly to the top phase.
- Partition coefficients of solutes tend to decrease at high solute concentrations.

Table 2. List of reagents and components used in the development of the HT platform, as well as their supplier and respective purities.

Reagents and components	Supplier	Purity
Polyethylene glycol 2000 g/mol	Merck (Darmstad, Germany)	-
Polyethylene glycol 4000 g/mol	Merck (Darmstad, Germany)	-
Polyethylene glycol 6000 g/mol	J.T. Baker (Fisher, New Jersey, USA)	-
Potassium citrate tribasic monohydrate ($K_3C_6H_5O_7.H_2O$)	Sigma Aldrich (Taufkirchen, Germany)	≥ 99 %
Potassium sodium tartrate tetrahydrate ($KNaC_4H_4O_6.4H_2O$)	Sigma Aldrich (Taufkirchen, Germany)	≥ 99 %
Sodium phosphate monobasic dehydrate ($NaH_2PO_4.2H_2O$)	Sigma Aldrich (Taufkirchen, Germany)	≥ 95 %
Ammonium citrate dibasic ($(NH_4)_3C_6H_5O_7$)	Honeywell Fluka (Buchs, Switzerland)	≥ 99 %

Sodium tartrate dehydrate ($Na_2C_4H_4O_6.2H_2O$)	Sigma Aldrich (Taufkirchen, Germany)	≥ 99 %
Magnesium sulphate heptahydrate ($MgSO_4.7H_2O$)	J.T. Baker (Fisher, New Jersey, USA)	-
Potassium dihydrogen phosphate (KH_2PO_4)	Merck (Darmstad, Germany)	≥ 99 %
Sodium sulphate (Na_2SO_4)	Merck (Darmstad, Germany)	≥ 99 %
Potassium phosphate dibasic (K_2HPO_4)	Honeywell Fluka (Buchs, Switzerland)	≥ 99 %
Sodium succinate dibasic hexahydrate ($Na_2C_4H_6O_4.6H_2O$)	Sigma Aldrich (Taufkirchen, Germany)	≥ 99 %
Potassium oxalate monohydrate ($K_2C_2O_4.H_2O$)	Honeywell Fluka (Buchs, Switzerland)	≥ 99 %
Tri-Sodium citrate dihydrate ($Na_3C_6H_5O_7.2H_2O$)	Merck (Darmstad, Germany)	≥ 99 %
Anhydrous glucose	Sigma Aldrich (Taufkirchen, Germany)	-
Sodium carbonate (Na_2CO_3)	Sigma Aldrich (Taufkirchen, Germany)	≥ 99 %
3,5-Dinitrosalicylic acid (DNS)	Sigma Aldrich (Taufkirchen, Germany)	≥ 98 %
Methyl violet	Merck (Darmstad, Germany)	-

Table 2. Range of salt and polymer concentrations used to determine phase diagrams (at 40 °C) in the HT platform.

PEG MW	Reliable experimental area	
	Salt [% (w/w)]	Polymer [% (w/w)]
2000	10 to 25	3 to 25
4000	5 to 19	3 to 25
6000	1 to 20	1 to 25

Table 3. Deviation of the protein mass measured in top and bottom phase in relation to the total mass of protein added in the system (mass balance deviation), for different tie line lengths

(TLL). The measured protein concentration was 0.3 g/L ± 0.03, 0.6 g/L ± 0.03 and 0.9 g/L ± 0.06, respectively to the enzymatic loads of 5, 10 and 15 PFU/g bagasse. The values are represented in percentage.

Protein load (FPU/g bagasse)	PEG 6000-potassium citrate pH5			PEG 2000-magnesium sulphate pH5		
	TLL 34.2 %	TLL 35.9%	TLL 38.1%	TLL 38.0%	TLL 40.2%	TLL 42.2%
5	29 ± 8	17 ± 8	15 ± 8	27 ± 7	27 ± 7	29 ± 8
10	41 ± 5	44 ± 5	48 ± 5	27 ± 4	32 ± 4	39 ± 5
15	47 ± 5	46 ± 5	56 ± 5	39 ± 5	35 ± 5	49 ± 5

Table 4. Deviation of the sugar mass measured in top and bottom phase in relation to the total mass of sugar added in the system (mass balance deviation), for different tie line lengths (TLL). The values are represented in percentage.

Sugar load (g/L)	PEG 6000-potassium citrate pH5			PEG 2000-magnesium sulphate pH5		
	TLL 34.2 %	TLL 35.9%	TLL 38.1%	TLL 38.0%	TLL 40.2%	TLL 42.2%
29 ± 0.3	9 ± 4	6 ± 4	15 ± 4	3 ± 4	2 ± 4	1 ± 4
51 ± 0.5	21 ± 2	37 ± 3	34 ± 3	14 ± 2	16 ± 2	16 ± 2
61 ± 0.6	28 ± 3	34 ± 3	38 ± 3	13 ± 4	7 ± 4	11 ± 4

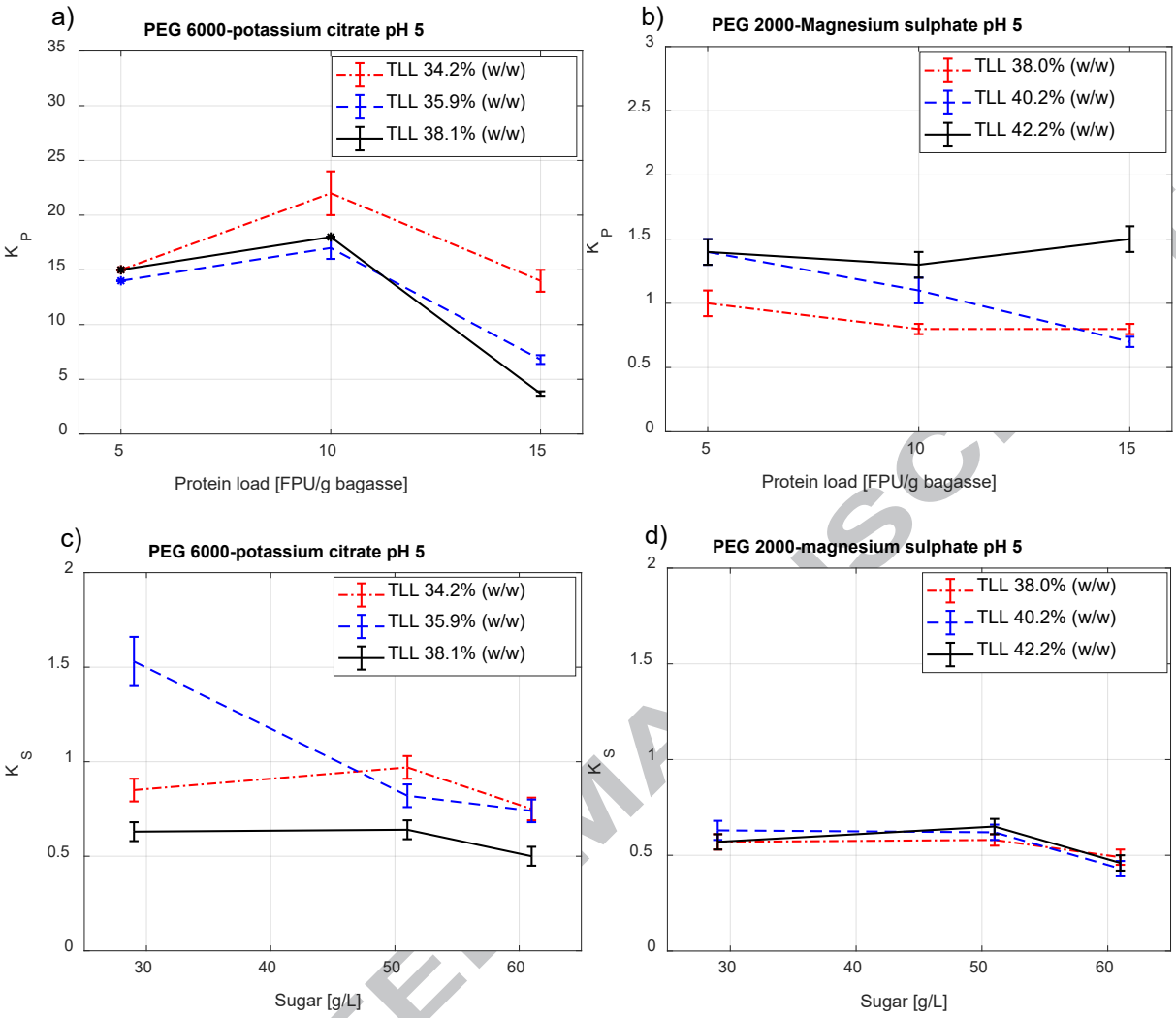

Fig. 6

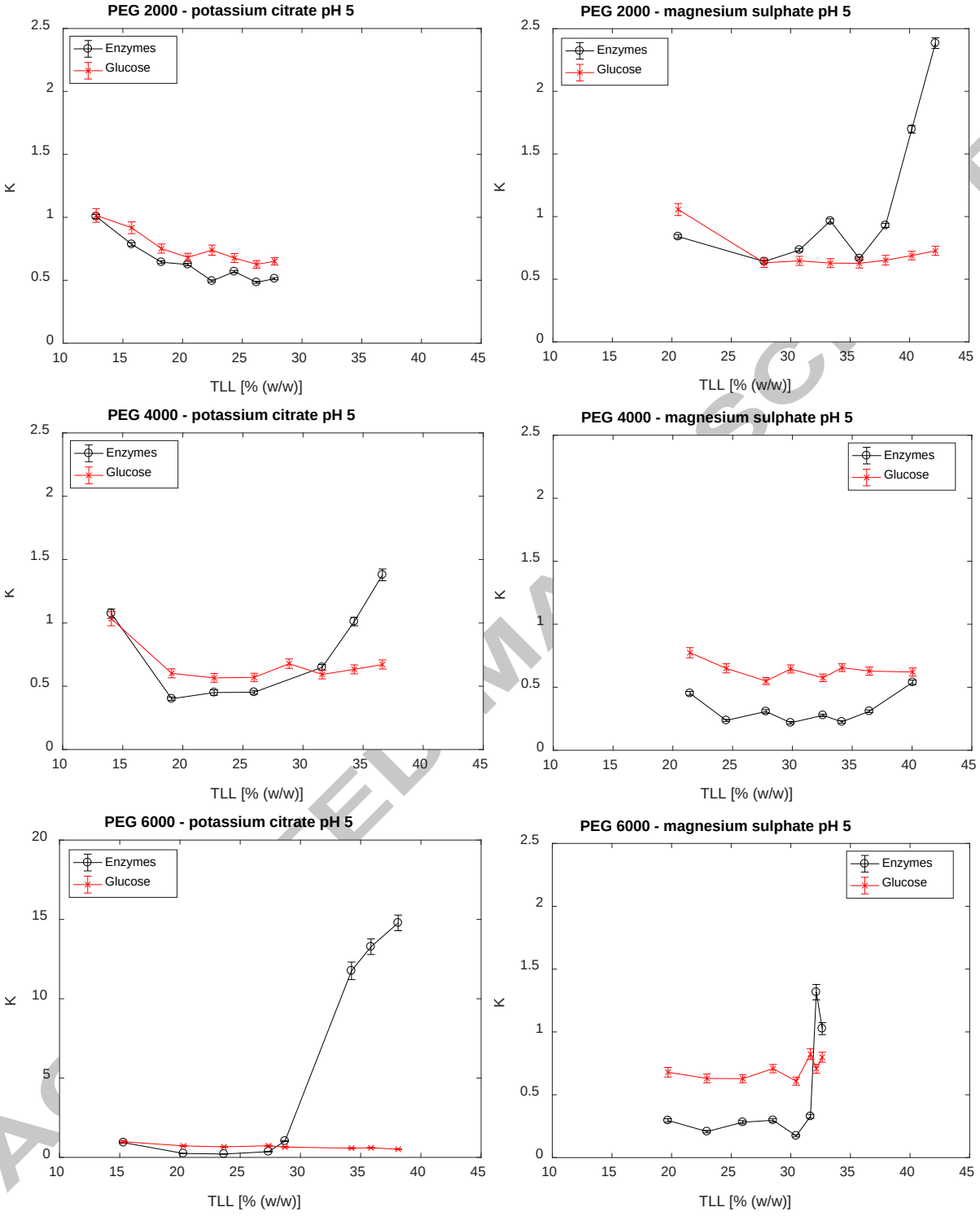

Fig. 5

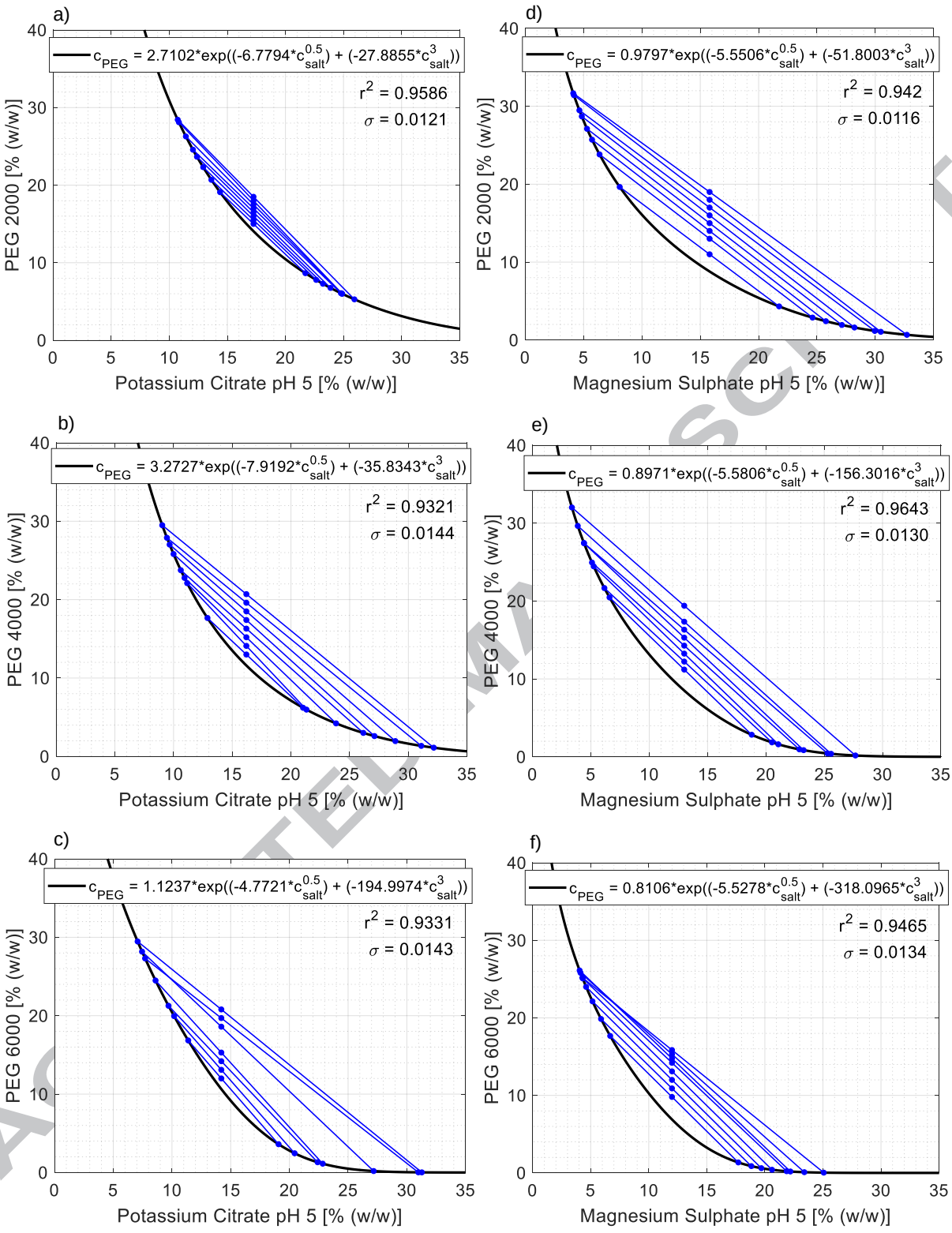

Fig. 4

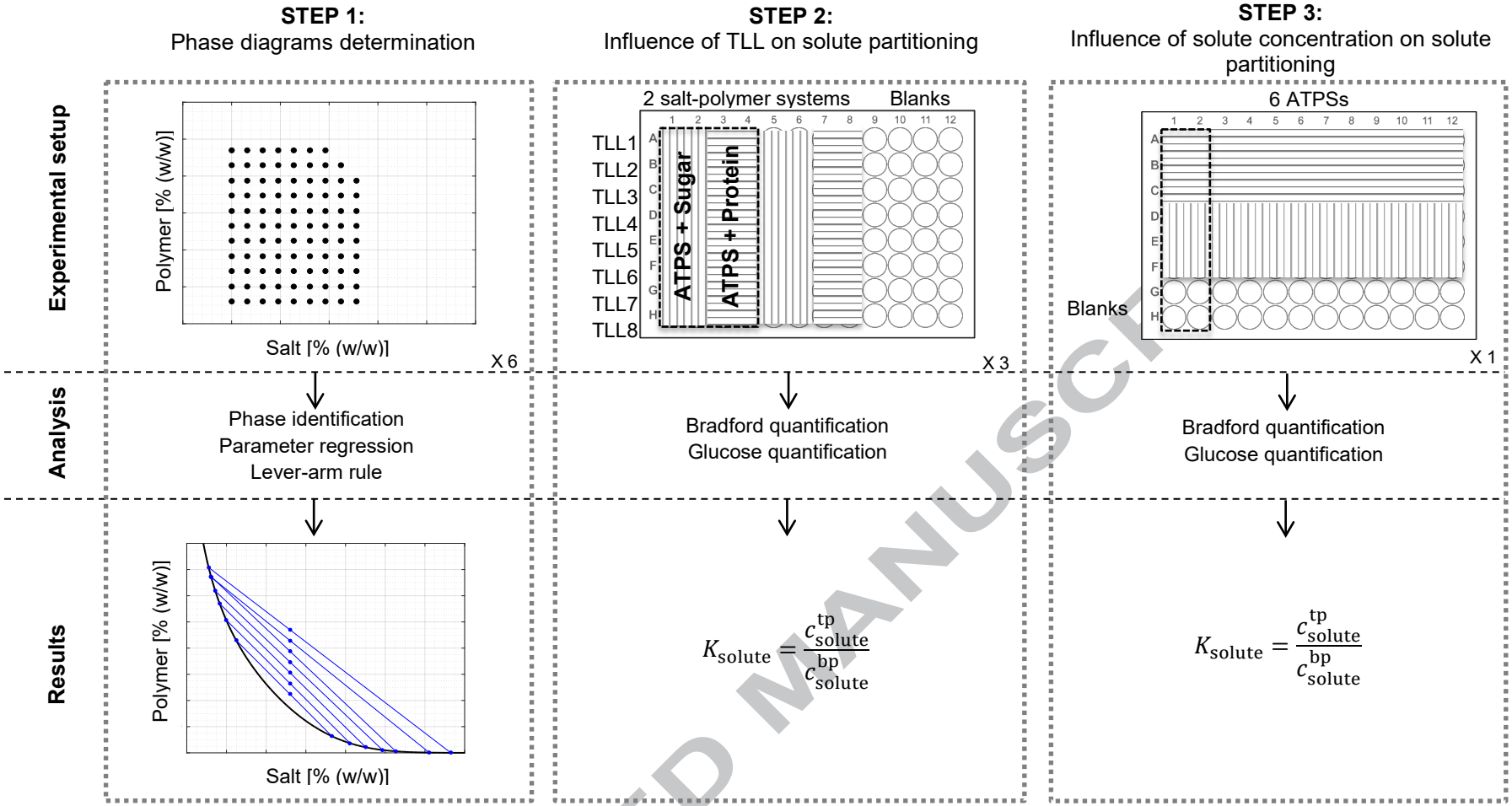

Fig. 3

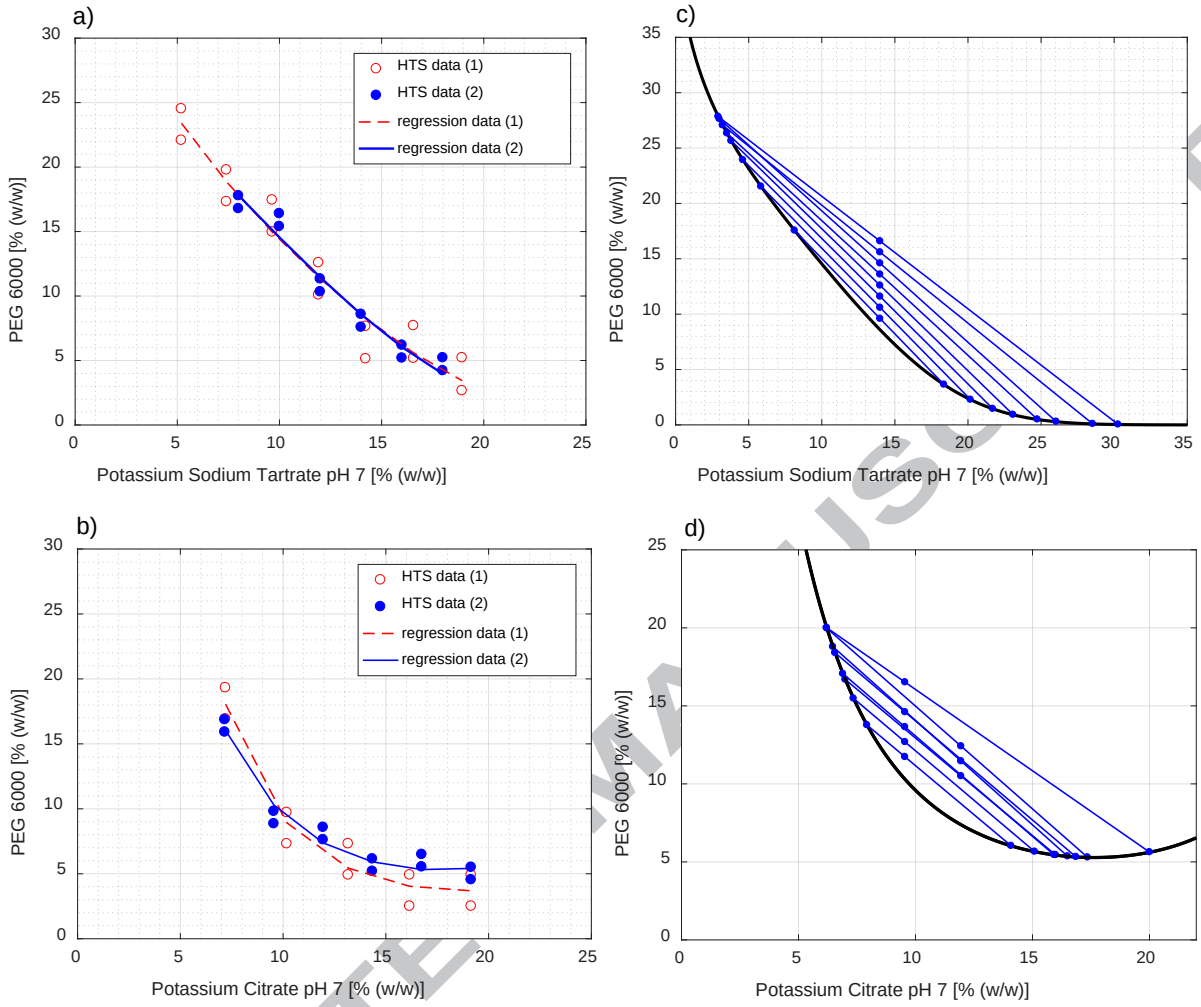

Fig. 2

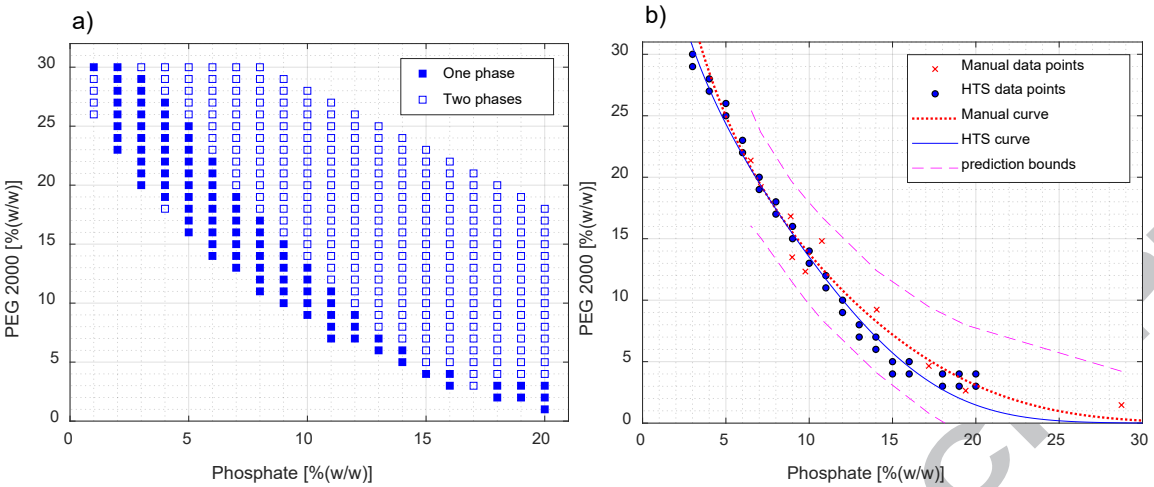

Fig. 1.